I. INTRODUCTION

Recently, synthesis of nano-particles with a uniform size and shape have shown interesting properties particularly nanocrystalline of metal oxides, due to its numerously important properties such as catalytic, electrical and optical properties. Among them, ZnO is one of candidate materials which have been attracting attention because of its wide band gap energy of about 3.36 eV. Therefore, ZnO is an important material for room temperature UV lasers and short-wavelength optoelectronic device [1, 2]. Furthermore, ZnO with its good electrical and optical properties can be used in many applications such as photoconductors, integrated sensors and transparent conducting oxide electrodes [3, 4]. Up to now, a number of chemical routes have been used to synthesize nanocrystalline ZnO powders such as hydrothermal method [5], simple chemical route [6], spray pyrolysis [7] and sol-gel method [8]. Among these methods, chemical route shows many advantages over other techniques such as its simplicity and low equipment cost.

However, synthesis of nano-particles of metal oxides at low cost in industrial scale is a challenge in material production. So, using the cheap materials, simple fabrication processes and suitable conditions of synthesis are the main requirement for this process. Therefore, the study of influence of various parameters such as initial solution combination, time and temperature of heat treatments, and type of surfactant is very important for nano-powders production.

The main purpose of the present research is to study the post-annealing temperature effect on structural, optical properties of ZnO nano powder and gas sensing performance of ZnO thick films synthesized by the simple chemical route.

II. EXPERIMENTAL PROCEDURE

a. Synthesis of ZnO nano-particles

ZnO nano-particles preparation by simple chemical route is summarized in a flow chart shown in figure 1. The precursor solution consisting of zinc acetate and citric acid dissolved in H_2O and methanol (1:1) separately with equal weight percentage is prepared and resulting mixture was stirred and dissolved at 60 ^oC for 30 min until a completely clear solution was obtained then pH of the solution was brought to 8.5 by drop wise addition of ammonium hydroxide solution (25%).

of organic part to inorganic part is kept in range of 25:75 during formulating the paste. The thick film prepared by screen printing technique in which paste is robbed on screen printing machine. The uniform film is formed by applying uniform pressure. The film then fired at 550^{o}C to remove organic material. The gas sensitivity is measured for various gases like ethanol, H_2S, NH_3, LPG, Cl_2, CO, CO_2, H_2 and O_2.

d. Characterization of powders

The X-ray diffraction (XRD) patterns of ZnO nano-particles prepared at various annealing temperatures were recorded by the D8 Advance Bruker system using CuKα radiation with 2θ in the range 20–80^{o}. Transmission electron microscopy (TEM) micrographs and electron diffraction patterns of the prepared ZnO nano-particles were recorded by the Make Philips Model CM-200 (Specification: operating voltage 20-200 kV, resolution 2.4 Å. The required samples for TEM analysis was prepared by dispersing the ZnO nano-particles in ethanol using an ultrasonic bath. A drop of this dispersed suspension was put onto 200-mesh carbon coated Cu grid and then dried under UV lamp. Also, the optical absorption measurements of nano-particles in range of 200-700 nm were recorded using a UV–VIS spectrophotometer (Schimadzu-2450) for calculating optical band gap values. The surface morphology of thick films was analyzed by using a scanning electron microscope [SEM model JEOL 2300 Japan].

III. RESULTS AND DISCUSSION

a. XRD analysis

The XRD patterns of prepared ZnO nano-particles at different annealing temperatures are shown in figure 2. It is clear that the powder which is annealed at 500^{o}C is slightly crystalline with a less intensity. Those annealed at 700 and 900 ^{o}C are well crystallized. All the diffraction peaks well matches with the standard JCPDS data of ZnO with card no. 36-1451. Also, the Bragg's peaks of the crystallized powders correspond to each sample agree well with the reflections of ZnO with a = 3.242 Å and c = 5.176 Å. The XRD patterns at all annealing temperatures show that the higher intensities of three basic peaks of the (1 0 0), (0 0 2), (1 0 1) and (1 1 0) planes are more than of other peaks.

crystalline peak at the angular range of 36.2- 36.4°.

Table 1 shows the different XRD parameters for all the films. It can be seen that the percentage of crystallinity and grain size systematically increased with increase in annealing temperature. Similar reports of increase in crystallinity with different annealing temperature can be seen in literature [12]. Interplanar and interchain distances were marginally changed because the angle of the peak (θ) did not vary significantly. Also the lattice strain decreases with increase in annealing temperature.

Table 1. The XRD parameters and mean grain size at different annealing temperatures.

Annealing temp. (^{o}C)	**Peak angle θ (degree)**	**Degree of crystallinity *Dc* (%)**	**Grain size *t* (nm)**	**Interplanar distance *d* (Å)**	**Interchain distance *r* (Å)**	**Lattice strain *g* (%)**
500	18.2	62.30	16	2.4684	0.7845	0.23
700	18.2	73.22	18	2.4702	0.8127	0.20
900	18.2	96.59	21	2.4728	0.8454	0.13

b. TEM analysis

The TEM micrographs of the ZnO powders annealed at different temperatures are shown in figure 3. The TEM images confirm the nanometric size of the particles in the range of 8, 14 and 18 nm depending on the annealing temperature 500, 700 and 900^{o}C respectively. Figure 3(a) exhibits nano-sized ZnO particles inside a dark background due to the organic additives maintenance, i.e. citric acid, in the powder. By increasing the annealing temperatures nano-particles are observed well, as shown in figure 3(b)–(c). In addition, the morphology of ZnO nano-particles strongly depends on the annealing temperatures, so that in higher temperatures, especially in T= 900 ^{o}C, the size of nano- particles is increased, as shown in figure 3(c). The TEM micrograph of powders also shows a well distribution of nano-particles in powders.

Table 2: *d* values obtained from XRD and TEM.

Reported d values (Å)	**X-ray diffraction (XRD) d values (Å)**	**Electron diffraction (TEM)**		**Planes (*hkl*)**
		Reciprocal of d values δhkl (nm^{-1})	***d values dhkl Å***	
2.8143	2.8117	3.90	2.5641	(1 0 0)
2.6033	2.6049	4.24	2.3640	(0 0 2)
2.4759	2.4728	4.37	2.2883	(1 0 1)
1.9111	1.9088	5.60	1.7857	(1 0 2)
1.6247	1.6248	6.43	1.5552	(1 1 0)
1.4771	1.4764	7.09	1.4104	(1 0 3)
1.3582	1.3775	7.58	1.3192	(1 1 2)

c. SEM analysis

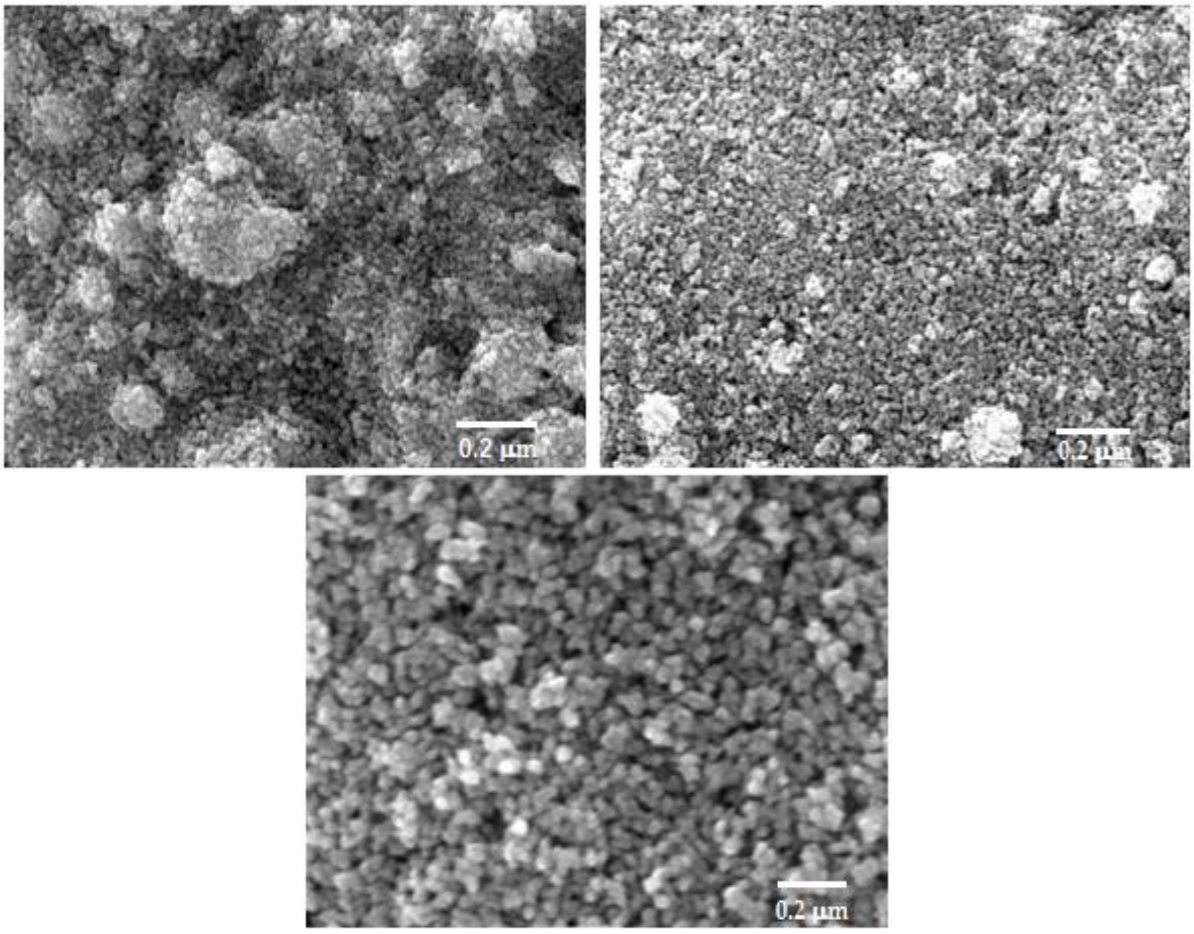

Figure 4. SEM photographs of ZnO thick films at annealing temperature (a) 500^{o}C, (b) 700^{o}C and (c) 900^{o}C.

properties necessary for gas sensor application. The dependence of the sensitivity of the ZnO thick films to 10 ppm of H_2S at annealing temperature 500^{o}C, 700^{o}C and 900^{o}C on the operating temperature is shown in figure 5. The sensitivity is found to be maximum when the annealing temperature was 700^{o}C. The annealing in air renders more oxygen vacancy generation, which enhances the gas sensitivity. It is observed that the sensitivity increases 50^{o}C to 200^{o}C and then decreases with the further increase in the operating temperature. It showed the maximum sensitivity of 123, 376 and 95 to 10 ppm of H_2S at annealing temperatures 500^{o}C, 700^{o}C and 900^{o}C respectively.

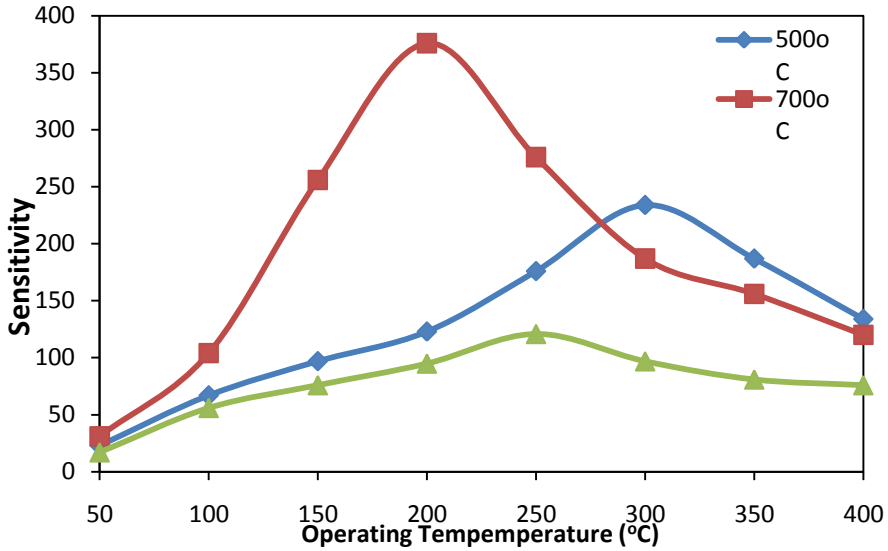

Figure 5. Effect of annealing temperature on the sensitivity of ZnO thick films to 10 ppm of H_2S gas.

b. Variation in sensitivity with H_2S gas concentration

The dependence of the sensitivity of ZnO thick films on the H_2S concentration at an operating temperature 200^{o}C is shown in figure 6. It is observed that the sensitivity increases linearly as the H_2S concentration increases from 1 to 10 ppm and then decreases with further increase in the H_2S concentration. The linear relationship between the sensitivity and the H_2S concentration at low concentrations may be attributed to the availability of sufficient number of sensing sites on the film to act upon the H_2S. The low gas concentration implies a lower surface coverage of gas molecules, resulting into lower surface reaction between the surface adsorbed oxygen species and the gas molecules. The increase in the gas concentration increases the surface reaction due to a large surface coverage. Further increase in the surface reaction will be gradual when saturation of

It is observed from figure 7 that ZnO thick films gives maximum sensitivity to H_2S (10 ppm) at 200°C. The films showed highest selectivity for H_2S against all other tested gases: NH_3, LPG, Cl_2, CO, CO_2, O_2, H_2 and ethanol. The selectivity also increases with annealing temperature.

d. Response time and recovery time

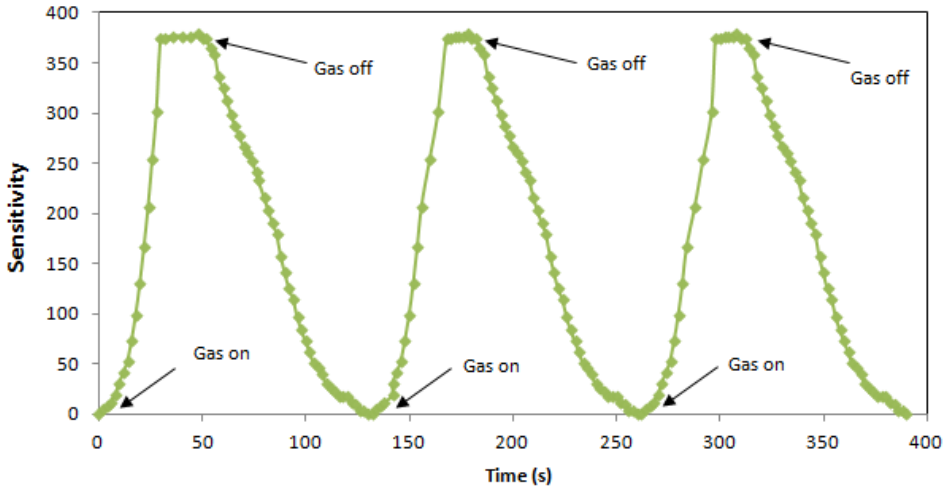

Figure 8. Response and recovery of ZnO thick films.

The response and recovery of ZnO thick films annealed at 700°C are represented in figure 8. The response was quick (~30 s) even to a trace amount (10 ppm) of H_2S gas, while the recovery was fast (~76 s). The quick response may be due to faster oxidation of gas. The negligible quantity of the surface reaction product and its high volatility explains its quick response and fast recovery to its initial chemical status. These results indicate that the ZnO prepared by spray pyrolysis method is a suitable material for the fabrication of the H_2S sensor. A number of experiments have been carried out to measure the sensitivity as a function of the operating temperature. All the time the sensitivity of the sensor element has approximately constant values, indicating the repeatability of the sensor.

e. H_2S-sensing mechanism

According to the present understanding on the response of semiconductor gas sensors, the change in the electrical resistance is closely related to the chemical properties of the surface oxygen. In the aerial atmosphere where the partial pressure of oxygen is taken as constant, oxygen is adsorbed on ZnO surfaces in different forms depending on the temperature, usually

When the dominating species that is O_2^-, the equation describing its interaction with H_2S on ZnO surface can be written as

$$H_2S(gas) \rightarrow H_2S(ads) \quad (7)$$

$$H_2S(ads) + O_2^- \rightarrow SO_2(gas) + H_2\,(gas) + e^- \quad (8)$$

Application of the mass action law to (5) and (6) gives

$$[H_2S\,(ads)] = K_{H_2S}P_{H_2S} \quad (9)$$

$$[e^-] = K_1[H_2S\,(ads)][O_2^-][SO_2]^{-1}[H_2]^{-1}$$

$$= K_1K_{H_2S}P_{H_2S}\,[O_2^-][SO_2]^{-1}[H_2]^{-1} \quad (10)$$

where K_{H_2S} and K_1 are the equilibrium constants of (7) and (8), P_{H_2S} is the concentration of H_2S gas in air, and the bracketsmeanthe concentration per unit area. The electrical resistance (Rg) is inversely proportional to $[e^-]$ so that we obtain

$$Rg \propto (K_1K_{H_2S}P_{H_2S})^{-1}[O_2^-]^{-1}[SO_2][H_2] \quad (11)$$

Inserting this into (8) where Ra is irrelevant to P_{H_2S} gives the response

$$S = Ra/Rg \propto P_{H_2S} \quad (12)$$

Similarly, when the dominating species that participating in the reaction is O^-, we obtain

$$H_2S(ads) + 2O^- \rightarrow SO_2(gas) + H_2(gas) + 2e^- \quad (13)$$

$$[e^-]^2 = K_2K_{H_2S}P_{H_2S}\,[O^-]^2[SO_2]^{-1}[H_2]^{-1} \quad (14)$$

$$Rg \propto (K_2K_{H_2S}P_{H_2S})^{-0.5}[O^-]^{-1}[SO_2]^{0.5}[H_2]^{0.5} \quad (15)$$

$$S = Ra/Rg \propto P_{H_2S}{}^{0.5} \quad (16)$$

When the dominating species that participating in the reaction is O^{2-}, we obtain

$$H_2S(ads) + 2O^{2-} \rightarrow SO_2(gas) + H_2(gas) + 4e^- \quad (17)$$

$$[e^-]^4 = K_3K_{H_2S}P_{H_2S}\,[O^{2-}]^2[SO_2]^{-1}[H_2]^{-1} \quad (18)$$

$$Rg \propto (K_3K_{H_2S}P_{H_2S})^{-0.25}[O^{2-}]^{-0.5}[SO_2]^{0.25}[H_2]^{0.25} \quad (19)$$

$$S = Ra/Rg \propto P_{H_2S}{}^{0.5} \quad (20)$$

where K_2 and K_3 are the equilibrium constants of (13) and (17).

Therefore, the dependence of the response on gas concentration can be characterized by the power law

$$S \propto P_{H_2S}{}^{m} \quad (21)$$

been observed for the sensor samples prepared from three different kinds of ZnO nano-particles toward H_2S gas in the range 10–100 ppm.

V. CONCLUSIONS

The ZnO nano-particles were synthesized successfully by simple chemical route accompanied by citric acid as a surfactant. From XRD and SEM analysis, it is confirmed that grain size systematically increased with increase in annealing temperature. The TEM images confirm the nanometric size of the particles in the range of 8, 14 and 18 nm depending on the annealing temperature 500, 700 and 900^oC respectively. The maximum sensitivity was obtained at an operating temperature of 200^oC for the exposure of 10 ppm of H_2S over other gases with quick response (30 s) and fast recovery (76 s) for ZnO thick film prepared from powder annealed at 700 ^oC.

ACKNOWLEDGEMENT

Authors are very much thankful to the Principal, Arts, Commerce and Science College, Nandgaon, Principal, KTHM College, Nashik for providing laboratory facilities and UGC, New Delhi financial help for this research work.

REFERENCES

[1] D. Bao, H. Gu and A. Kuang, “Sol-gel-derived c-axis oriented ZnO thin films”, Thin Solid Films, Vol. 312, 1998, pp. 37-39.

[2] S. B. Majumdar, M. Jain, P. S. Dobal and R. S. Katiyar, “Investigations on solution derived aluminium doped zinc oxide thin films”, Mat. Sci. Eng. B, Vol. 103, 2003, pp. 16-25.

[3] Y. Huang, M. Liu, Z. Li, Y. Zeng and S. Liu, “Raman spectroscopy study of ZnO-based ceramic films fabricated by novel sol-gel process”, Mat. Sci. Eng. B, Vol. 97, 2003, pp. 111-6.

[4] J. Xu, Q. Pan, Q. Shun and Z. Tian, "Grain size control and gas sensing properties of ZnO gas sensor", Sensor. Actuat. B-Chem., Vol. 66, 2000, pp. 277-279.

[5] U. Pal, P. Santiago, G. Xiong, K. B. Ucer and R. T. Williams, "Synthesis and optical properties of ZnO nanostructures with different morphologies", Opt. Mater., Vol. 29, 2006, pp. 65-69.

[6] S. D. Shinde, G. E. Patil, D. D. Kajale, V. B. Gaikwad and G. H. Jain, "Gas sensing performance of nanostructured ZnO thick film resistors", International Journal of Nanoparticles (Article in Press).

[7] M. T. Mohammad, A. A. Hashim and M. H. Al-Maamory, "Highly conductive and transparent ZnO thin films prepared by spray pyrolysis technique", Mater. Chem. Phys., Vol. 99, 2006, pp. 382-287.

[8] H. Tang, M. Yan, X. Ma, H. Zhang, M. Wang and D. Yang, "Gas sensing behavior of polyvinylpyrrolidone-modified ZnO nanoparticles for trimethylamine", Sensor. Actuat. B-Chem., Vol. 113, 2006, pp. 324-328.

[9] S. Chattopadhy, T. K. Chaki, A K Bhowmick, Structural characterization of electron-beam crosslinked thermoplastic elastomeric films from blends of polyethylene and ethylene-vinyl acetate copolymers, J. Appl. Polym. Sci., 81, 2001, pp. 1936–1950.

[10] B. D. Cullity, Elements of X-ray diffraction, Addison-Wesley Publishing Co., 1956.

[11] L. E. Alexander, X-ray diffraction methods in polymer science, Wiley Interscience, New York, 1980.

[12] S. A. Ketabi, A. S. Kazemi and M. M. Bagheri-Mohagheghi, "The effect of complexing agent on the crystallization of ZnO nanoparticles", Pramana- Journal of Physics, Vol. 77, No. 4, 2011, pp. 679–688.

[13] G. E. Patil, D. D. Kajale, S. D. Shinde, V. B. Gaikwad and G. H. Jain, "Synthesis and characterization of SnO_2 nanoparticles by hydrothermal route for gas sensing application" International Nano Letters Vol. 2, No. 1, January 2012, pp. 46-51.

[14] Y. Shimizu, M. Egashira, Basic aspects and challenges of semiconductor gas sensors, MRS Bulletin, 24, 6, 1999, pp. 18–24.

[15] N. Yamazoe, Toward innovations of gas sensor technology, Sensors and Actuators B, 108, 1-2, 2005, pp. 2–14.

[16] G. H. Jain, G. E Patil, D. D. Kajale and V. B. Gaikwad, "Cr_2O_3-doped $BaTiO_3$ as an Ammonia Gas Sensor", New Developments and Applications in Sensing Technology, Lecture Notes in Electrical Engineering, 2011, Volume 83, pp. 157-167.

[17] G. H. Jain, L. A. Patil, V. B. Gaikwad, Studies on gas sensing performance of $(Ba_{0.8}Sr_{0.2})(Sn_{0.8}Ti_{0.2})O_3$ thick film resistors, Sensors and Actuators B: Chemical, 122, 2007, pp. 606-612.

[18] T. Seiyama, A. Kato, K. Fujiishi, M. Nagatani, A new detector for gaseous components using semiconductive thin films, Analytical Chemistry, 34, 11, 1962, pp. 1502–1503.

[19] D. N. Chavan, V. B. Gaikwad, D. D. Kajale, G. E. Patil, G. H. Jain, "Nano Ag-doped In_2O_3 thick film: A low temperature H_2S gas sensor", Journal of Sensors, Volume 2011, Article ID 824215, 8 pages doi:10.1155/2011/824215.

[20] S.C. Chang, "Oxygen chemisorption on tin oxide: correlation between electrical conductivity and EPR measurements", J. Vac. Sci. Technol., Vol. 19, 1980, pp. 366–369.

[21] N. Barsan, U.Weimar, "Conduction model of metal oxide gas sensors", J. Electroceram., Vol. 7, 2001, pp. 143–167.